Supporting Information

Insight into Structural Change of ABA-Type Amphiphilic Block Copolymers during Sol-Gel Transition Using Infrared Spectroscopy and Near-Infrared Spectroscopy

Chongwen Xiong,[a,&] Biao Ma,[b,&] Teng Qiu,[a,c] Xiaoyu Li,[a,c] Xueguang Shao,[b,*] Longhai Guo[a,c,*]

a. State Key Laboratory of Organic-Inorganic Composites, Beijing University of Chemical Technology, Beijing 100029, PR China

b. Research Center for Analytical Sciences, College of Chemistry, Nankai University, Tianjin 300071, PR China

c. Beijing Engineering Research Center of Synthesis and Application of Waterborne Polymer, Beijing University of Chemical Technology, Beijing 100029, PR China

E-mail address: guolh@mail.buct.edu.cn (L. Guo), xshao@nankai.edu.cn (X. Shao).

&. These authors contributed equally to this work and should be considered co-first authors

This PDF file includes:

Supporting Information 1: The synthetic route of copolymers, GPC analysis and ^{1}H-NMR analysis.

Supporting Information 2: Definition of elasticity index (EI), comparison of microrheology and bulk rheology and supplementary TEM Photos.

Supporting Information 3: The illustration information about genetic algorithm and figure of GA fitting curve.

Supporting Information 4: Supplementary IR spectra, second derivative curves and 2D-COS analysis.

Supporting Information 5: NIR supplementary information.

Supporting Information 1: The synthetic route of copolymers, GPC analysis, ^{1}H-NMR analysis

Synthesis of PDMAA-*b*-PDAAM-*b*-PDMAA Triblock Copolymers

The synthetic route of PDMAA-*b*-PDAAM-*b*-PDMAA is shown in the Figure S1.

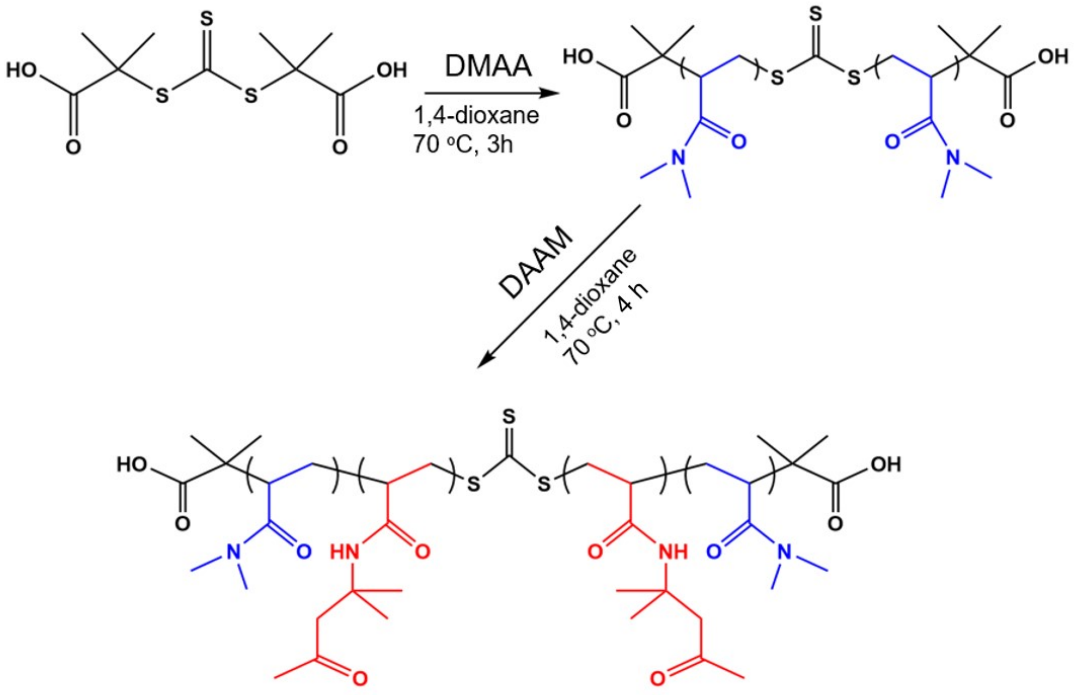

Scheme S1. Synthetic schematic diagram of PDMAA-CTA and PDMAA-*b*-PDAAM-*b*-PDMAA.

^{1}H-NMR and GPC analysis

The ^{1}H nuclear magnetic resonance (^{1}H-NMR) spectra were recorded using a Bruker AVANCE III 400MHz NMR spectrometer.

The peak m is the characteristic peak of trioxane and the peak e is the characteristic peak of methyl of PDMAA. Through their respective integral strengths, NMR characterization molecular weight can be obtained by the formation

$$M_{PDMAA} = \frac{Ie}{Im} \times M_{DMAA} + M_{BDAAT} \quad (1)$$

M_{PDMAA} = 4426 by calculating and the DP of PDMAA is approximately 40. The disappearance of the monomer double bond peak in the NMR figure shows each polymerization conversion rate is over 99%.

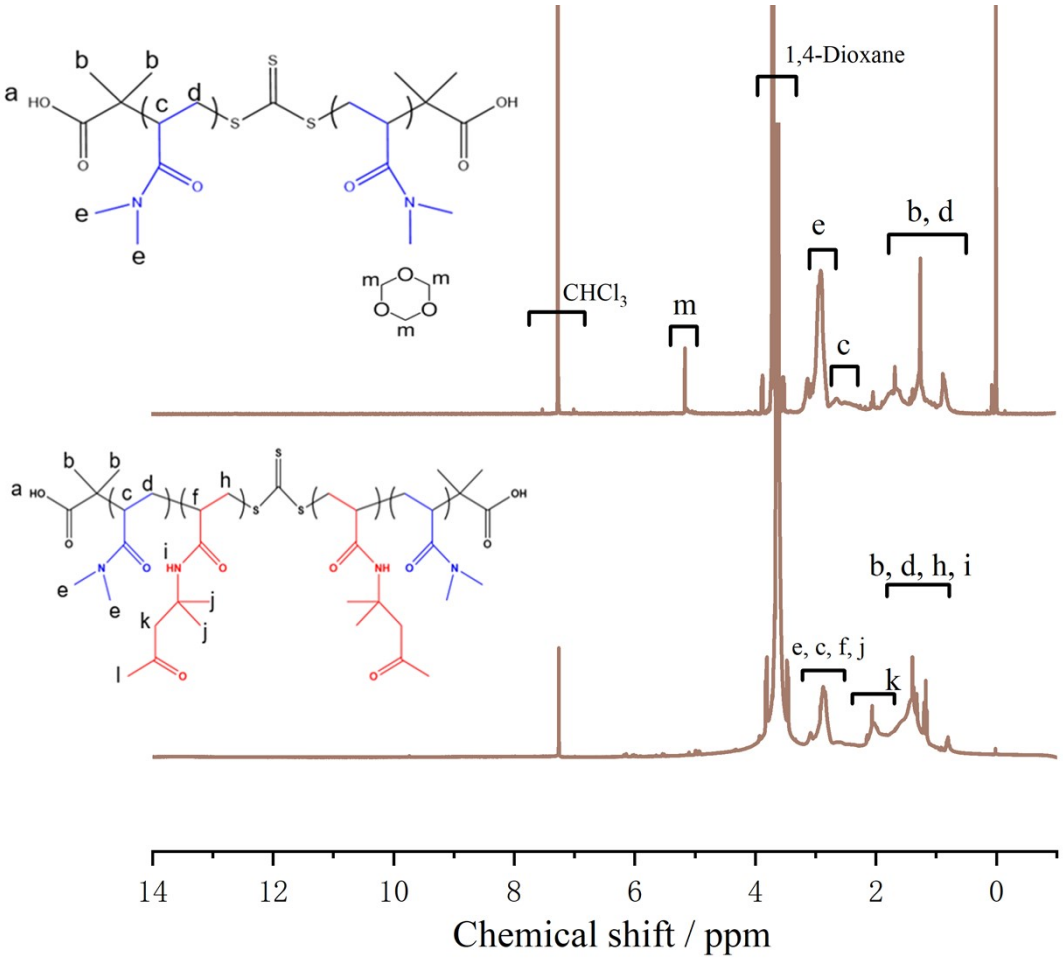

Figure S1. [1] H NMR spectra recorded in $CDCl_3$ for (a) $PDMAA_{40}$-CTA, (b) PDMAA-*b*-PDAAM-*b*-$PDMAA_{20}$

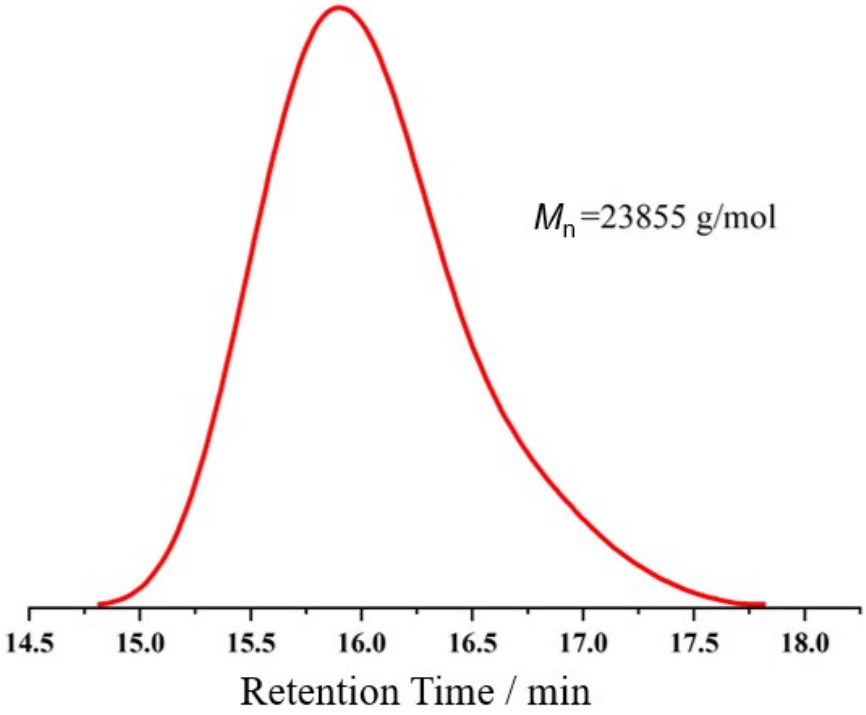

Figure S2. DMF GPC data for PDMAA-*b*-PDAAM-*b*-PDMAA.

Supporting Information 2: Definition of elasticity index (EI), comparison of microrheology and bulk rheology and supplementary TEM Photos

Calculation of EI in microrheology

The elasticity index is an automatically calculated parameter. The specific formula for calculating EI is as follows:

$$EI = \frac{1}{6\delta^2} \cdot \frac{de}{d} \quad (2)$$

where $6\delta^2$ (nm^2) is the mean value of MSD at the decorrelation time interval is 2.5 ms to 1.5 s, d (μm) is the mean particle diameter measured by laser diffraction, and d_e is the diameter of a model particle used for calibration (d_e = 1 μm).

Comparison of microrheology and bulk rheology

In order to compare the microrheological data and bulk rheology, we performed the bulk rheological experiment on our synthesized ABA-type tri-block copolymer. For rheological measurement, the evolution of storage modulus (G') and loss modulus (G'') of the hydrogel as functions of temperature from 38 to 55 °C were recorded by using an MCR301 torque rheometer (Anton Paar, Austria), with 25 mm parallel plates and a gap size of 1.0 mm. The evolution of G' and G'' as a function of temperature are plotted in Figure S3a. The strain and the frequency are 1% and 1 rad/s, respectively.

The variation MSD can be obtained as a function of time (τ), and based on the Stokes-Einstein equation,[1] we can calculate both G' and G'' as a function of frequency. Selecting a fixed frequency, G' and G' can be also directly calculated from the MSD curve as a function of temperature. The fixed frequency is 1 rad/s which is consistent

with the bulk rheological frequency. G' and G'' as a function of temperature is plotted in Figure S3b.

As shown in Figure Sa and b, for the comparison of G' and G'' measured by bulk rheometer and microrheology, the variation trends are exactly the same, indicating that both of them can obtain the same rheological characteristics of the gel. For the comparison between G' and EI measured by bulk rheology and microrheology, respectively, almost the same temperature region of the gelation transition can be obtained. Therefore, the microrheological result is almost consistent with the bulk rheological results, although the values of EI and G' are different.

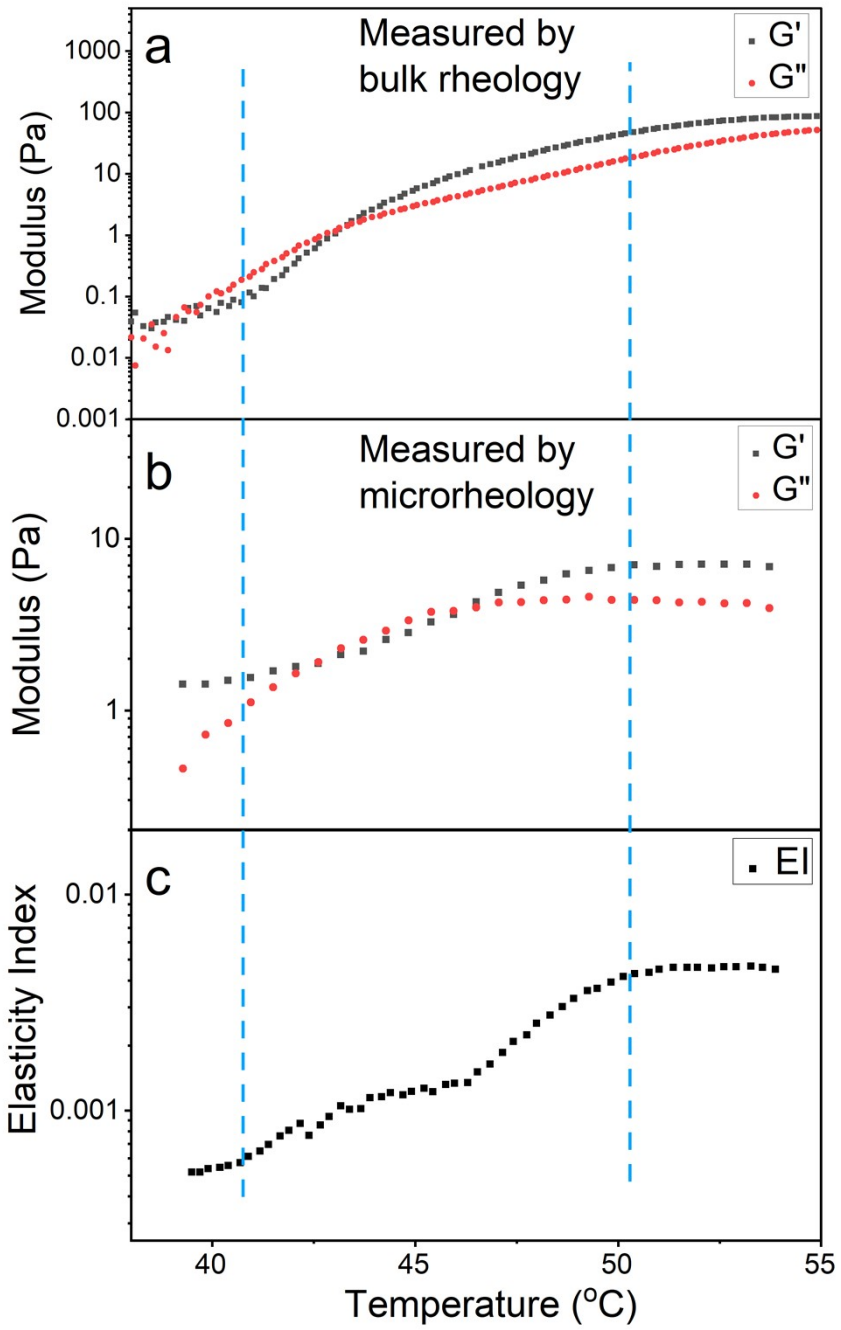

Figure S3. (a) Plots of *G*' and *G*' as a function of temperature measured by torque rheometer; (b) *G*' and *G*" calculated from the MSD curve; (c) EI from MSD curve.

Supplementary TEM photos

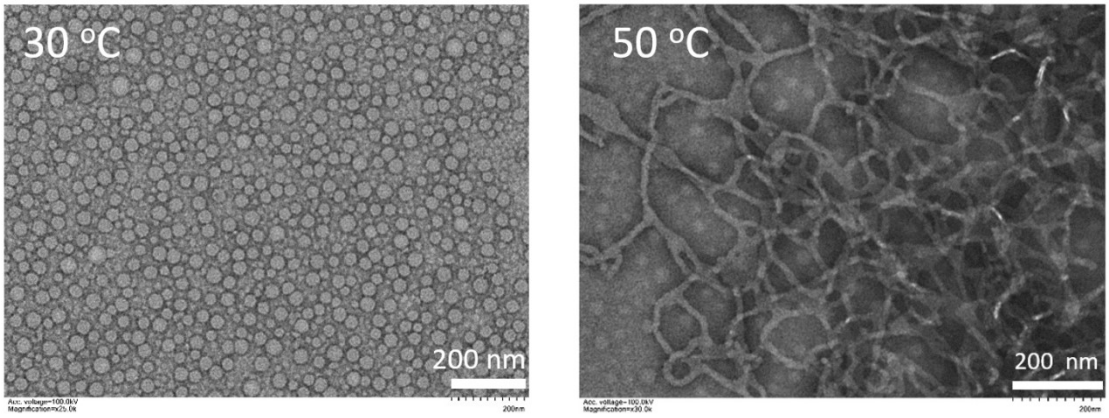

Figure S4. Spherical micelles at low temperature and worm-like micelles at high temperature.

TEM samples were prepared at 30 °C and 50 °C, respectively. The copolymer dispersion with a solid content of 20 wt% was maintained at the specified temperature and the tool for preparing the sample was placed at the same temperature. After the dispersion is stabilized, dilute the 20 wt% solution in pure water to 0.5 wt%. The samples were placed in an ultrasonic water bath at the same temperature for 20s. The diluted dispersion is transparent. The samples were picked up with a TEM copper mesh and then treated with 2 wt% phosphotungstic acid for negative staining. The different morphologies at different temperatures were observed and recorded using a Hitachi HT7700 transmission electron microscope.

Supporting Information 3: The illustration information about genetic algorithm and figure of GA fitting curve

Gaussian peak via genetic algorithm was performed to fit the IR spectrum. To obtain a better fitting result, a single-peak Gaussian function was used to represent the absorption band of a single component, and the overlapping absorption peaks were decomposed into a linear combination of multiple Gaussian peaks. More illustrations about genetic algorithm can be seen in support information.

The expression of Gaussian multimodal fitting is

$$y = y_0 + \sum_{i=1}^{n} \frac{b_n}{w_n\sqrt{2}} e^{-\frac{(x-\lambda_n)^2}{2w_n^2}} + e \quad \textbf{(3)}$$

The formula consists of two parts: the spectral baseline (y_0) and the probability density formula of the single-peak Gaussian function. Among them, λ_i is the peak position of the *i*-th Gaussian peak (the wavelength at the maximum absorbance), ω_i is the half-width of the *i*-th Gaussian peak, b_i represents the combination coefficient corresponding to the *i*-th Gaussian peak, and *e* represents the Gaussian multimodal the residual spectrum after fitting.

In order to facilitate analysis, the 1750-1570 cm^{-1} band is selected as the research object of peak splitting. For eliminating the interference of baseline drift, the two-point method is used to subtract the baseline background information of the 1750-1570 cm^{-1} band. The peak position is determined by second-derivative curves. Thus, n=5 was used to describe the spectral bands. The chromosome is consisted of 10 ($2\times n$) genes, determining the position and the width of seven peaks. The deviations for the two parameters encoded in the genes were set as [–4, +4] and [-8, +8], respectively.

The results of genetic algorithm fitting at 40 °C are plotted in Figure S4, which shows the successful fitting of IR spectra in the range of 1750-1570 cm^{-1}.

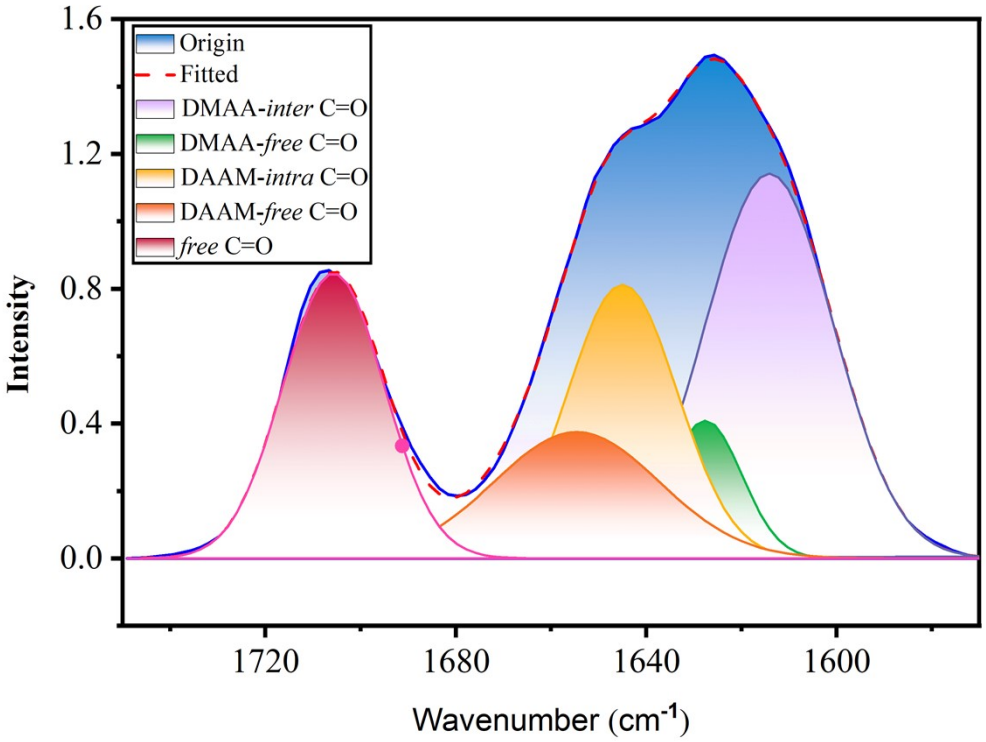

Figure S5. Gaussian fitting curve at 45 °C by five peaks.

Supporting Information 4: Supplementary IR spectra, second derivative curves and 2D-COS analysis

The spectra of C-H bands

The spectra of PDMAA, PDAAM, and PDMAA-*b*-PDAAM-*b*-PDMAA powder is shown in Figure S5. The bands at 2975 cm^{-1} belong to PDAAM and is considered as the CH groups of CH_3. The copolymer solution shows a slightly blueshift of the spectra at 2975 cm^{-1}. However, the copolymer powder at different temperatures shows no difference. Moreover, the wavenumber of solution spectra is higher than that of powder spectra, which may cause by the hydration of PDAAM block in solution.

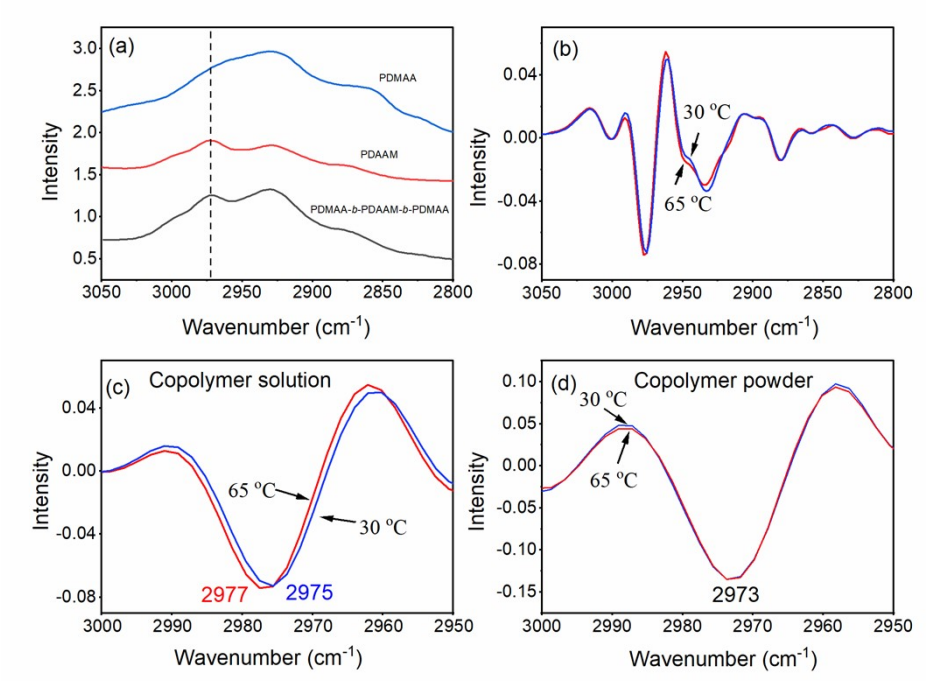

Figure S6. (a) The IR spectra of PDMAA, PDAAM, PDMAA-*b*-PDAAM-*b*-PDMAA powder in C-H bands; The second derivative curves of PDMAA-*b*-PDAAM-*b*-PDMAA solution of (b) 30 and 65 °C at 3050 to 2800 cm^{-1}, (c) the

magnified range of 3000 to 2950 cm^{-1}; and (d) the second derivative curves of PDMAA-*b*-PDAAM-*b*-PDMAA powder at 30 and 65 °C for a comparison.

IR spectra of PDMAA and PDAAM

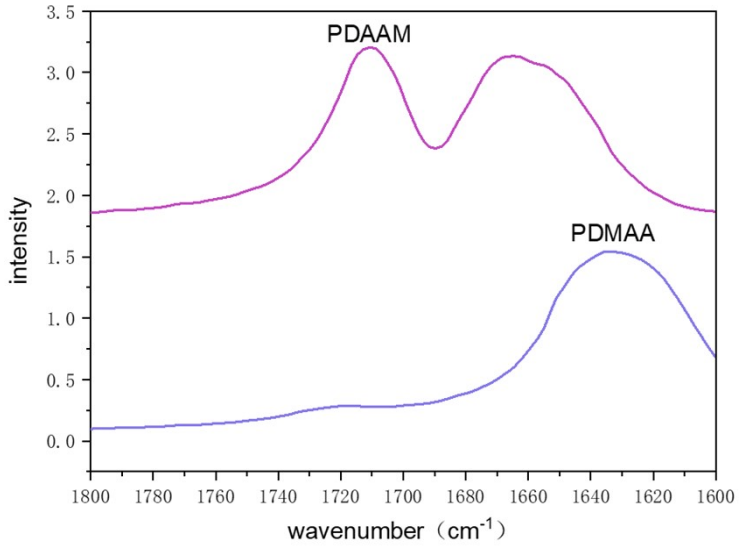

Figure S7. The FTIR spectrum of homopolymer (a) PDMAA and (b) PDAAM

2D-COS analysis of IR spectra

In order to understand the sequential order of each group in the gelation process, 2D-COS first proposed by Noda[2] is used to expand the spectra in two dimensions to improve the spectral resolution. Asynchronous spectrum can also separate overlapping peaks. 2D-COS of ν(N-H) and ν(C=O) regions are obtained and shown in Figure S6. In the synchronous spectrum, the peak on the diagonal is called the autocorrelation peak, which reflects the degree of spectral intensity change under external perturbations. The peak outside the diagonal in the asynchronization spectrum are called cross peak, which reflects whether there is a strong interaction or pairing between functional groups. Combining synchronous with asynchronous spectra can judge the sequence of changes of each component under external disturbance conditions according to Noda's rule. When cross-peaks (v_1,v_2) in the synchronous and asynchronous spectra hold the same

symbol, both positive or both negative, it can be inferred that peak v_1 changes prior to peak v_2 with the perturbation, whereas when cross-peaks (v_1, v_2) in the synchronous and asynchronous spectra hold different symbols, one positive and the other negative, it can be deduced that peak v_2 changes prior to peak v_1. The symbol of each peak can be seen in Table S1. In IR analysis, the bands at 1708 cm^{-1} does not change significantly with temperature changes and keeps stable during gelation process. Thus, the peaks change after 1708 will not analyze.

Table S1. Synchronous and Asynchronous 2D Correlation Intensities, $\Phi(\boldsymbol{v_1}, \boldsymbol{v_2})$ and $\Psi(\boldsymbol{v_1}, \boldsymbol{v_2})$, respectively, and the Sequential Order in the Temperature Variations of the Two Diffraction Peaks at $\boldsymbol{v_1}$ and $\boldsymbol{v_2}$.

$\Phi(v_1, v_2)$	$\Psi(v_1, v2)$	Sequantial order
Φ(3349, 3469)>0	**Ψ(3349,3451)>0**	**3351 after 3469**
Φ(1708, 1656)<0	**Ψ(1708, 1656)>0**	**1708 after 1656**
Φ(1708, 1647)>0	**Ψ(1708, 1647)<0**	**1708 after 1647**
Φ(1708, 1610)<0	**Ψ(1708, 1610)<0**	**1708 after 1610**
Φ(1656, 1647)<0	**Ψ(1656, 1647)<0**	**1656 before 1647**
Φ(1656, 1610)<0	**Ψ(1656, 1647)<0**	**1656 before 1610**
Φ(1708, 3469)<0	**Ψ(1708, 3469)>0**	**1708 after3469**
Φ(1708, 3349)<0	**Ψ(1708, 3349)>0**	**1708 after 3349**
Φ(1656, 3469)>0	**Ψ(1656, 3369)<0**	**1656 after 3469**
Φ(1656, 3349)>0	**Ψ(1656, 3349)>0**	**1656 before 3349**
Φ(1647, 3469)<0	**Ψ(1647, 3469)>0**	**1647 after 3469**
Φ(1647, 3349)<0	**Ψ(1647, 3349)>0**	**1647 after 3349**

Φ(1610, 3469)<0	**Ψ(1647, 3469)>0**	**1610 after 3469**
Φ(1610, 3349)<0	**Ψ(1610, 3349)>0**	**1610 after 3349**
Φ(2975, 1708)>0	**Ψ(2975, 1708)>0**	**2975 before 1708**
Φ(2975, 1610)>0	**Ψ(2975, 1610)<0**	**2975 after 1610**

The sequance order can be described as follow: 3469 > 1656 > 3349 > 1647 > 1610 > 2975> 1708 (> indicates that the previous one occurs first).

Supporting Information 5: NIR supplementary information

The intensity of the peak at 5954 cm^{-1} in transformed spectra

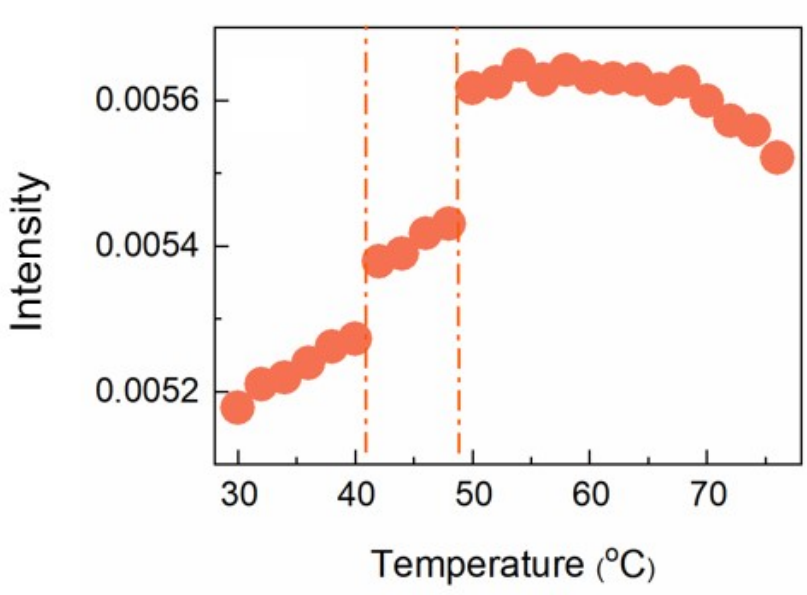

Figure S8. the variation of the spectral intensity at 5954 cm^{-1} with temperature for the PDMAA-*b*-PDAAM- *b*-PDMAA solution.

NPCA from 7200 to 6400 cm^{-1}

Temperature-dependent NIR and NPCA analysis on pure water was also performed as a comparison. Two PCs can explain more than 99.99% variance of the data. The time scores are relatively stable, and the concentration scores increase evenly in Figure S9. Time and concentration are considered not to affect the molecular structure in the studied range. The yellow and blue lines represent copolymer solution and pure water, respectively. The two lines are similar in PC1, PC2, and PC4. Including that those spectral contain the information of bulk water, bound water, and an intermediate state

of water from pure water, respectively. The loading of PC5 may contain background and interference information and will not be analyzed in this work.

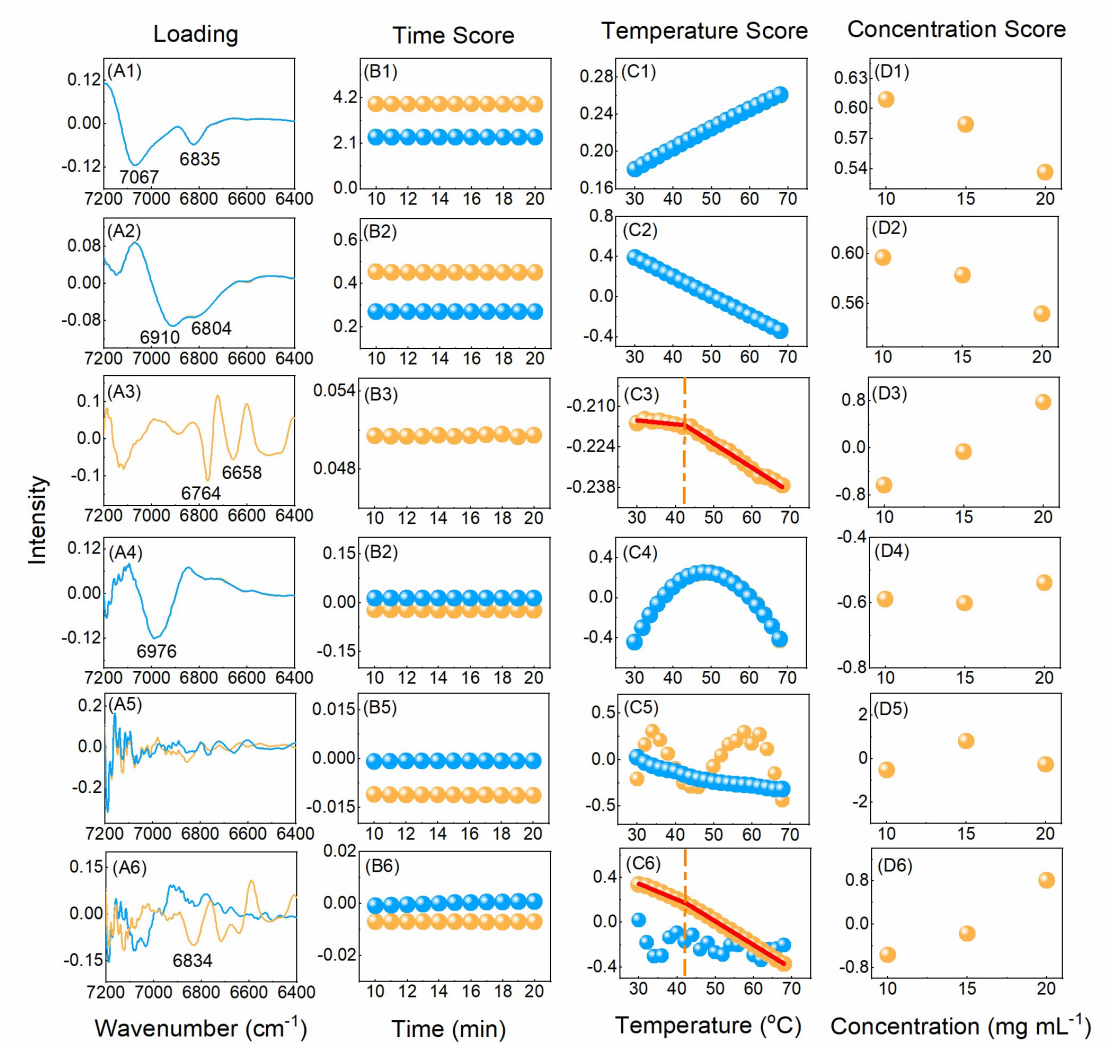

Figure S9. The first six PCs extracted by NPCA on the temperature-dependent NIR spectra of PDMAA-*b*-PDAAM-*b*-PDMAA solution from 7200 to 6400 cm^{-1}.

References

(1) C, Sekine. T. Uchiumi, I. Shirotani, et al. Metal-insulator transition in $PrRu_4P_{12}$ with skutterudite structure. *Phys. Rev. Lett.* 1997, 79(17): 3218.

(2) Noda, I. Generalized Two-Dimensional Correlation Method Applicable to Infrared, Raman, and Other Types of Spectroscopy. *Appl. Spectrosc*. **1993**, *47*, 1329-1336.